Distributed Control of Reactive Power from Photovoltaic Inverters*

Soumya Kundu
University of Michigan
Ann Arbor, MI 48105
Email: soumyak@umich.edu

Scott Backhaus
Los Alamos National Laboratory
Los Alamos, NM 87544
Email: backhaus@lanl.gov

Ian A. Hiskens
University of Michigan
Ann Arbor, MI 48105
Email: hiskens@umich.edu

***Abstract*—As new devices and technologies enter the electrical distribution grid, decentralized control algorithms will become increasingly important. Unlike centralized control where standard optimization procedures can ensure optimal system performance, control algorithms for distributed systems may take a variety of forms. This paper derives a decentralized algorithm that regulates the reactive power output from highly distributed photovoltaic (PV) sources. An objective function is constructed that minimizes voltage deviations and line losses. It is shown that this objective function is minimized by a local control law that regulates the reactive power output of PV inverters. Optimality of the derived control law is tested against central optimization solutions.**

I. Introduction

With increasing penetration of distributed generation units, it is important to devise ways of using their reactive power capability to improve the performance of the electrical grid. At the distribution level, residential photovoltaic (PV) generation is becoming popular, particularly in sunnier climates. A PV panel produces direct-current (DC) power, with production dependent upon the available solar irradiance. An inverter is required for connection to the AC grid. The rapid variations in PV power production can result in extensive voltage swings across the grid [1], [2], [3], [4]. However PV inverters are capable of providing reactive power support that can be used to stabilize grid voltages.

A relatively early study [5] considered opportunities for using the reactive power capability of distributed generators to provide grid support such as voltage regulation. The voltage sensitivity of lines to the dynamics of voltage-support distributed generators was analyzed in [2] to establish optimal design criteria. In [3], solar irradiance was described by a pseudo-random time series in order to assess the impact of fluctuating solar irradiance on grid voltages. High PV penetration at mid-voltage levels, under various loading and PV scenarios, was analyzed in [4] to determine the impact on network power loss, voltage balance and peak load compensation. Numerous control algorithms have recently been proposed for regulating the reactive power injection/consumption of the inverters associated with distributed PV sources. A *multi-agent system* based centralized dispatch scheme was developed in [6]. However to mitigate fast voltage fluctuations on distribution feeders, decentralized control schemes appear to provide a more viable option [7], [8], [9].

In [8], [9], local control schemes that are based on locally measurable variables, in particular the reactive power capability of the PV inverter and the local node voltage, were compared against a globally optimal centralized dispatch scheme. However the correlation between locally observable variables and the optimal reactive power dispatch has not yet been fully resolved, with further research required to formulate an optimal local control strategy. The approach adopted in this paper is to study the solutions of a global optimization problem for a wide variety of operating conditions, in particular loading and weather scenarios. Correlations between the optimal PV reactive power dispatch and locally measurable quantities such as voltage, power consumption and PV generation, are then used to motivate a near-optimal local control strategy.

*Research at Los Alamos National Laboratory was carried out under the auspices of the National Nuclear Security Administration of the U.S. Department of Energy, under Contract No. DE C52-06NA25396. Research was also supported by the National Science Foundation through the EFRI-RESIN grant 0835995.

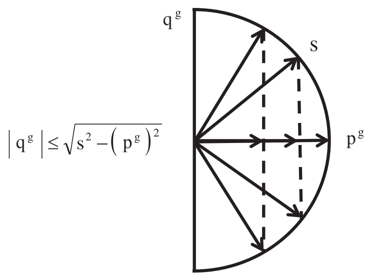

Fig. 1. Dependence of PV inverter reactive power capability q^g on active power generation p^g.

II. Model Description

A. PV inverters without storage

The active and reactive power generated by an inverter attached to the j-th PV source will be denoted by p_j^g and q_j^g, respectively. Without local storage, a PV inverter does not control p_j^g, but it can control q_j^g to be either positive or negative. This reactive power capability is limited by the inverter's fixed apparent power capability s_j and its variable active power generation p_j^g, and is given by [8], [10],

$$|q_j^g| \leq \sqrt{s_j^2 - (p_j^g)^2} := q_{j,max}^g. \quad (1)$$

This relationship is illustrated by the complex power diagram in Fig. 1. In [8], it was found that $s_j \approx 1.1p_{max}^g$ provides sufficient freedom in q_j^g to realize a substantial reduction in distribution losses. Under this condition, $|q_j^g| \leq 0.45p_{max}^g$ when $p_j^g = p_{max}^g$. The choice of $s_j \approx 1.1p_{max}^g$ is reasonable because inverters are available in discrete sizes and are likely to be slightly oversized relative to p_{max}^g. Throughout this paper, it is assumed that

$$p_{j,max}^g = 2 \text{ kW}, \quad s_j = 2.2 \text{ kVA}, \quad \forall j. \quad (2)$$

B. Grid model

This paper considers a distribution feeder structure that consists of a main line with no laterals, as shown in Fig. 2. The first node, at the substation, will be denoted node 0. Node number increases as the feeder is traversed away from the substation. The resistance and reactance between nodes i and $i+1$ are given by r_i and x_i, while

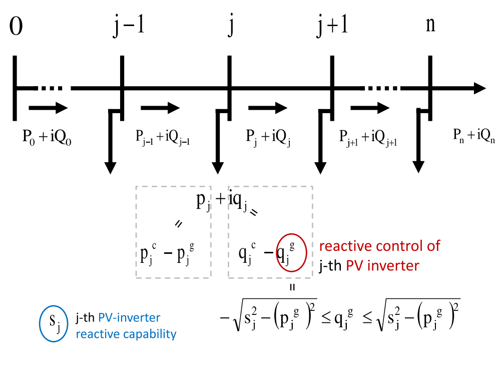

Fig. 2. Distribution feeder with no laterals.

P_i and Q_i denote the active and reactive power flowing from node i towards node $i+1$. The active and reactive power consumed at node i is given by p_i^c and q_i^c, and the active and reactive power generated by a PV source at node i is given by p_i^g and q_i^g.

Consider a distribution feeder with $N+1$ nodes, and with a PV source at each node. The feeder model can be written using the LinDistFlow form [11], [12], [13], where for each $i \in \{1, 2, ..., N\}$,

$$P_{i-1} = \sum_{j=i}^{N} p_j = \sum_{j=i}^{N} (p_j^c - p_j^g) \tag{3a}$$

$$Q_{i-1} = \sum_{j=i}^{N} q_j = \sum_{j=i}^{N} (q_j^c - q_j^g) \tag{3b}$$

$$V_i = V_0 - \sum_{j=0}^{i-1} (r_j P_j + x_j Q_j)\,. \tag{3c}$$

This set of equations provides a simplified and approximate load flow computation. Assuming small line losses, the equations are quite accurate and provide appealing optimization properties.

C. Generating scenarios

Five levels of loading (L1-L5) will be considered, with the active load at each node p_j^c drawn from a uniform distribution that has mean and width,

L1: 0.625 kW and 1.25 kW,
L2: 0.9375 kW and 1.875 kW,
L3: 1.25 kW and 2.5 kW,
L4: 1.5625 kW and 3.125 kW,
L5: 1.875 kW and 3.75 kW.

In each of these scenarios, the reactive load at each node q_j^c is drawn from a uniform distribution with mean value of $0.25p_j^c$ and a width of $0.1p_j^c$. For each of the five loadings, three different solar irradiance conditions are considered,

1) *Sunny*: all PV systems are generating at $p_j^g = p_{j,max}^g$.
2) *Night time*: all PV systems generate $p_j^g = 0$.
3) *Partly cloudy*: the PV system at the first node away from the substation is assigned either $p_j^g = 0.2p_{j,max}^g$ or $p_j^g = p_{j,max}^g$ with equal probability, and each subsequent node is assigned,

$$p_{j+1}^g = \begin{cases} p_j^g, & \text{with probability } 0.9 \\ p_{j+1,max}^g \left(1.2 - \dfrac{p_j^g}{p_{j,max}^g}\right), & \text{with probability } 0.1. \end{cases} \tag{4}$$

For each combination of loading and solar irradiance, twenty realizations were considered by randomly generating p_j^g, q_j^g, p_j^c, q_j^c. The line parameters r_j were drawn from a uniform distribution with range $0.66\ \Omega$ to $0.99\ \Omega$, and $x_j = 1.15r_j$.

III. Central Optimization

For all $j \in \{0, 1, \ldots, N\}$ define,

$$\Delta V_j := V_j - 1 \tag{5a}$$

$$\Delta V_j^{eff} := \begin{cases} 0, & |\Delta V_j| \le V_{sl} \\ \Delta V_j - V_{sl}, & \Delta V_j > V_{sl} \\ \Delta V_j + V_{sl}, & \Delta V_j < -V_{sl} \end{cases} \tag{5b}$$

where V_{sl} is a soft limit for the voltage deviations from 1.0 pu. The desired control objective is expressed though the following minimization,

$$\min_{q_j^g, V_0} \ \mathbb{M}\left(q_{j\ge1}^g; V_0\right) = \sum_{j=1}^{N} \left(\Delta V_j^{eff}\right)^2 + \sum_{j=0}^{N-1} r_j (P_j^2 + Q_j^2) \tag{6}$$
$$\text{s.t.,} \quad |V_j| \le 1.05, \quad \forall\, j \ge 0$$
$$|q_j^g| \le \sqrt{s_j^2 - (p_j^g)^2}, \quad \forall\, j \ge 1.$$

In most distribution systems, the maximum allowable deviation of the voltage V_j from 1.0 pu is 0.05. For subsequent investigations, the soft limit will be set to $V_{sl} = 0.02$. This allows the optimal control the latitude to minimize losses when the voltages V_j are well within normal bounds, while smoothing the control action as the voltages begin to significantly deviate from 1.0 pu. It is also assumed that the substation voltage V_0 can be adjusted.

The central optimization (6) was evaluated for 20 instances of each of the 15 cases discussed in Section II-C. The goal was to identify any correlation between the optimal q_j^g values and the locally observable (to the PV-node) quantities V_j, p_j^c, p_j^g, and q_j^c. Notice though that the load flow equations in (3) suggest that the q_j^g values are directly linked with the reactive power flow in the system, which directly affects the voltage profile on the feeder. Thus a strong correlation is expected between q_j^g and the locally observable variables q_j^c and V_j. Figs. 3(a)-3(b) show that some correlations exist between q_j^g and the local variables V_j and q_j^c. Red dots correspond to the q_j^g that encounter their limit defined in (1) while black dots show those q_j^g that are within their limit. Careful investigation reveals that q_j^g is generally affine with q_j^c, with a slope that is approximately 1. Also q_j^g increases or decreases linearly as V_j deviates from its nominal value of 1 pu by more than $V_{sl} = 0.2$ pu. It remains fairly independent of any voltage deviations that are within the soft bounds.

IV. Local Control Strategy

The imperfect correlations in Fig. 3 suggest that q_j^g is often set to q_j^c when the voltage deviations $(V_j - 1)$ are within soft limits, while responding linearly to voltage deviations beyond soft limits, $|V_j - 1| - V_{sl}$. This apparent strong correlation between the optimal q_j^g and the locally observable q_j^c and V_j motivates a local control law of the form,

$$q_j^g = q_j^c - \alpha \Delta V_j^{eff}, \quad \forall\, j \ge 1 \tag{7}$$

where α is a design parameter chosen to optimize q_j^g. It is shown in Theorem 1 that if the ratio of line reactance and line resistance is constant over the entire feeder, the control law in (7) is optimal with $\alpha = x_j/r_j$. Fig. 3(c) illustrates the correlation between $q_j^g - q_j^c$ and V_j. Setting α to $x_j/r_j = 1.15$, which follows from the line parameter choice in Section II-C, the suggested control law (7) closely replicates this observed correlation.

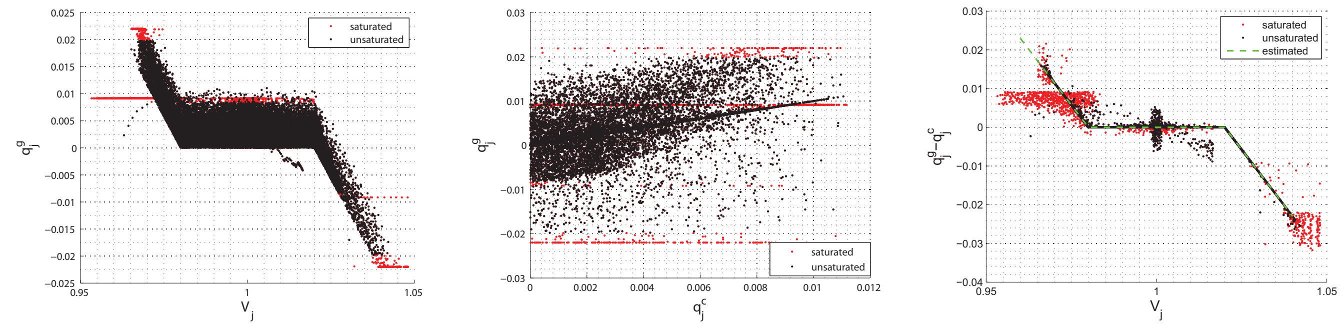

(a) (b) (c)

Fig. 3. Correlations between the local observables V_j and q_j^c and the optimal reactive dispatch q_j^g.

Theorem 1 (Optimality of the local control law): If all line impedances satisfy,

$$\frac{x_j}{r_j} = \alpha, \quad \forall j \in \{0, 1, 2, \dots, N-1\}, \tag{8}$$

where α is a constant, then the optimal q_j^g values that minimize the objective function (6) can be computed by observing only the local variables V_j and q_j^c, and are given by,

$$q_j^g = q_j^c - \alpha \Delta V_j^{eff}, \quad \forall\ j \geq 1. \tag{9}$$

Proof: It is assumed, for simplicity, that V_0 is set by some external method and hence is beyond the regime of local control action. From (3) and (5a), it can be written

$$\frac{\partial Q_j}{\partial q_k^g} = \begin{cases} 0, & k \leq j \\ -1, & k \geq j+1 \end{cases} \tag{10a}$$

and

$$\frac{\partial \Delta V_j}{\partial q_k^g} = -\sum_{i=0}^{j-1} x_i \frac{\partial Q_i}{\partial q_k^g} = -\sum_{i=0}^{\min(j,k)-1} x_i \frac{\partial Q_i}{\partial q_k^g} \tag{10b}$$

where the second equality in (10b) follows from (10a). Furthermore, it is shown in the Appendix that,

$$\frac{\partial \left(\Delta V_j^{eff}\right)^2}{\partial q_k^g} = 2\Delta V_j^{eff} \frac{\partial \Delta V_j}{\partial q_k^g}, \quad \forall\ j \geq 0, \forall\ k \geq 1. \tag{11}$$

The optimal values of q_j^g are given by the stationary points of (6),

$$f_k := \frac{\partial \mathbb{M}(q_{j\geq 1}^g; V_0)}{\partial q_k^g} = 0, \quad \forall k = \{1, 2, \dots, N\} \tag{12a}$$

which implies

$$\begin{aligned} f_k &= 2\left(\sum_{j=1}^{N} \Delta V_j^{eff} \frac{\partial \Delta V_j}{\partial q_k^g} + \sum_{j=0}^{N-1} r_j Q_j \frac{\partial Q_j}{\partial q_k^g}\right) \\ &= 2\left(-\sum_{j=0}^{N} \Delta V_j^{eff} \sum_{i=0}^{\min(j,k)-1} x_i \frac{\partial Q_i}{\partial q_k^g} - \sum_{j=0}^{k-1} r_j Q_j\right) \\ &= 0, \quad \forall\ k \geq 1. \end{aligned} \tag{12b}$$

Optimal q_N^g can be solved using f_N and f_{N-1}. From (12b), $f_N - f_{N-1} = 0$ implies,

$$-2\Delta V_N^{eff}\left(\sum_{i=0}^{N-1} x_i \frac{\partial Q_i}{\partial q_N^g} - \sum_{i=0}^{N-2} x_i \frac{\partial Q_i}{\partial q_{N-1}^g}\right) - 2r_{N-1}Q_{N-1} = 0$$

and using (10a) gives,

$$\Delta V_N^{eff}\left(\sum_{i=0}^{N-1} x_i - \sum_{i=0}^{N-2} x_i\right) - r_{N-1}Q_{N-1} = 0$$

$$\Rightarrow \quad Q_{N-1} = \frac{x_{N-1}}{r_{N-1}} \Delta V_N^{eff} \tag{13a}$$

$$\Rightarrow \quad q_N^g = q_N^c - \frac{x_{N-1}}{r_{N-1}} \Delta V_N^{eff} \tag{13b}$$

where the final step follows from (3). Thus the optimal q_N^g can be computed using only the local V_N and q_N^c, and satisfies the control law in (7) with $\alpha = x_{N-1}/r_{N-1}$.

The remainder of the proof follows from induction. It will be shown that if there exists an $M \in \{1, 2, \dots, N-1\}$ such that for all $k \geq M+1$,

$$q_k^g = q_k^c - \frac{x_{k-1}}{r_{k-1}} \Delta V_k^{eff} \tag{14a}$$

then,

$$q_M^g = q_M^c - \frac{x_{M-1}}{r_{M-1}} \Delta V_M^{eff}. \tag{14b}$$

It has already been shown in (13b) that there is an $M = N-1$ for which (14a) holds. To prove (14b), refer back to (12b), from which $f_M - f_{M-1} = 0$ implies,

$$-2\sum_{j=M}^{N} \Delta V_j^{eff}\left(\sum_{i=0}^{M-1} x_i \frac{\partial Q_i}{\partial q_M^g} - \sum_{i=0}^{M-2} x_i \frac{\partial Q_i}{\partial q_{M-1}^g}\right) - 2r_{M-1}Q_{M-1} = 0.$$

Using (10a), this gives,

$$Q_{M-1} = \frac{x_{M-1}}{r_{M-1}} \sum_{j=M}^{N} \Delta V_j^{eff}$$

and hence from (3),

$$\sum_{j=M}^{N} \left(q_j^c - q_j^g\right) = \frac{x_{M-1}}{r_{M-1}} \sum_{j=M}^{N} \Delta V_j^{eff}$$

$$\Rightarrow \quad q_M^g = q_M^c - \frac{x_{M-1}}{r_{M-1}} \Delta V_M^{eff} \tag{15}$$

where the final step makes use of (14a) and (8). Hence the claim in (14) is proved. The claim (14) together with (13b) complete the proof that each optimal q_j^g can be computed by observing local variables V_j and q_j^c, and its optimal value is given by (7) with $\alpha = x_{j-1}/r_{j-1}$. $\square$

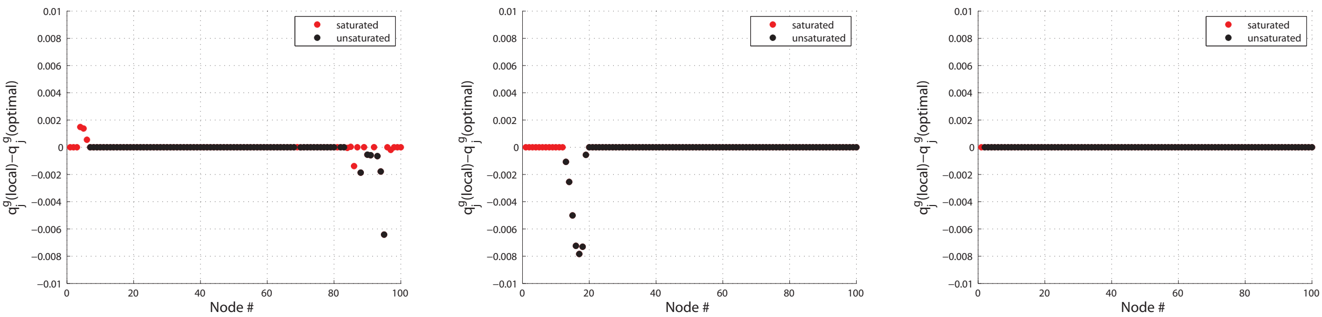

(a) (b) (c)

Fig. 4. Testing optimality of the local control law in - (a) *high import*, (b) *high export*, and (c) *balanced* situation.

V. RESULTS

Fig. 4 provides a comparison of the local control law (7) and the central optimization (6), for three distinct cases, 1) a *high import* case, Fig. 4(a), when the substation is supplying large active power to the feeder, 2) a *high export* case, Fig. 4(b), when the feeder is returning large active power back to the substation, and 3) a *balanced* situation, Fig. 4(c), when the generation from the PVs is almost balanced with the load consumption. It can be observed that the local control law almost always matches the optimal values, except when it has to compensate for neighboring PV sources that have encountered their limits, as seen in the extremities of Figs. 4(a) and 4(b).

VI. CONCLUSION

This paper undertakes a preliminary study to identify a decentralized control algorithm that minimizes line losses and voltage deviations by optimally dispatching the reactive power of PV inverters. It has been shown that there exists a strong correlation between the globally optimal reactive power dispatch and locally measurable quantities, in particular node voltage, reactive power consumption and PV generation. The derived local control law performs well, and closely matches the central optimal solution. Further research is required to investigate more general situations though, including PV penetration less than 100%, non-uniform ratio of line reactance to resistance ratio, and feeders with high line losses.

APPENDIX

From the definition (5a),(5b),

$$\frac{\partial\left(\Delta V_j^{eff}\right)^2}{\partial q_k^g} = 2\Delta V_j^{eff}\frac{\partial \Delta V_j^{eff}}{\partial q_k^g}$$

$$= \begin{cases} 0, & |\Delta V_j| \leq V_{sl} \\ 2(\Delta V_j - V_{sl})\frac{\partial \Delta V_j}{\partial q_k^g}, & \Delta V_j > V_{sl} \\ 2(\Delta V_j + V_{sl})\frac{\partial \Delta V_j}{\partial q_k^g}, & \Delta V_j < -V_{sl} \end{cases}$$

$$\forall j \geq 0, k \geq 1.$$

But it also follows directly from (5b) that,

$$2\Delta V_j^{eff}\frac{\partial \Delta V_j}{\partial q_k^g} = \begin{cases} 0, & |\Delta V_j| \leq V_{sl} \\ 2(\Delta V_j - V_{sl})\frac{\partial \Delta V_j}{\partial q_k^g}, & \Delta V_j > V_{sl} \\ 2(\Delta V_j + V_{sl})\frac{\partial \Delta V_j}{\partial q_k^g}, & \Delta V_j < -V_{sl} \end{cases}$$

$$\forall j \geq 0, k \geq 1.$$

Hence the relation (11) holds.

ACKNOWLEDGMENTS

We wish to thank the participants of the "Optimization and Control for Smart Grids" LDRD DR project at Los Alamos National Laboratory and the Smart Grid Seminar Series at CNLS/LANL for numerous fruitful discussions.

REFERENCES

[1] A. F. Povlsen, "Impacts of Power Penetration from Photovoltaic Power Systems in Distribution Networks," *International Energy Agency*, Feb. 2002.

[2] M. A. Kashem and G. Ledwich, "Multiple Distributed Generators for Distribution Feeder Voltage Support," *IEEE Transactions on Energy Conversion*, vol. 20, pp. 676–684, Sep. 2005.

[3] A. Woyte, V. V. Thong, R. Belmans, and J. Nijs, "Voltage Fluctuations on Distribution Level Introduced by Photovoltaic Systems," *IEEE Transactions on Energy Conversion*, vol. 21, no. 1, pp. 202–209, Mar. 2006.

[4] J. V. Paatero and P. D. Lund, "Effects of large-scale photovoltaic power integration on electricity distribution networks," *Renewable Energy*, vol. 32, pp. 216–234, Feb. 2007.

[5] G. Jóos, B. Ooi, D. McGillis, F. Galiana, and R. Marceau, "The potential of distributed generation to provide ancillary services," in *Proc. IEEE PES Summer Meeting*, vol. 3, 2000.

[6] M. Baran and I. El-Markabi, "A multiagent-based dispatching scheme for distributed generators for voltage support on distribution feeders," *IEEE Transactions on Power Systems*, vol. 22, no. 1, pp. 52–59, Feb. 2007.

[7] A. D. Dominguez-Garcia and C. N. Hadjicostis, "Coordination and Control of Distributed Energy Resources for Provision of Ancillary Services," in *2010 First IEEE International Conference on Smart Grid Communications*, 2010.

[8] K. Turitsyn, P. Sulc, S. Backhaus, and M. Chertkov, "Distributed control of reactive power flow in a radial distribution circuit with high photovoltaic penetration," in *IEEE Power and Energy Society General Meeting*, Jul. 2010, pp. 1–6.

[9] ——, "Options for Control of Reactive Power by Distributed Photovoltaic Generators," in *Proceedings of the IEEE*, vol. 99, 2011.

[10] E. Liu and J. Bebic, "Distribution system voltage performance analysis for high-penetration photovoltaics," *NREL/SR-581-42298, Tech. Rep.*, Apr. 2008.

[11] M. Baran and F. Wu, "Optimal capacitor placement on radial distribution systems," *IEEE Transactions on Power Delivery*, vol. 4, no. 1, p. 725734, Jan. 1989.

[12] ——, "Optimal sizing of capacitors placed on a radial distribution system," *IEEE Transactions on Power Delivery*, vol. 4, no. 1, p. 735743, Jan. 1989.

[13] K. Turitsyn, P. Sulc, S. Backhaus, and M. Chertkov, "Local Control of Reactive Power by Distributed Photovoltaic Generators," in *1st IEEE Internationl Conference on Smart Grid Communications*, 2010.